Second-Harmonic Rayleigh Scattering from a Sphere of Centrosymmetric Material

J. I. Dadap,[1] J. Shan,[1] K. B. Eisenthal,[2] and T. F. Heinz[1]
[1]*Department of Physics, Columbia University, New York, New York 10027*
[2]*Department of Chemistry, Columbia University, New York, New York 10027*
(Received 17 June 1999)

We describe the electromagnetic theory of second-harmonic generation from the surface of a sphere that is small compared to the wavelength of light. In a leading-order expansion, the second-harmonic radiation is emitted in nonlocally excited electric dipole and locally excited electric quadrupole modes. We analyze the problem with particular emphasis on experimental aspects, such as the radiation pattern, polarization selection rules, determination of nonlinear susceptibilities, radiation efficiency, and spectral characteristics.

PACS numbers: 42.65.–k, 03.50.De, 52.35.Nx, 73.20.Mf

Second-harmonic generation (SHG) is a well-established surface-specific probe of centrosymmetric media [1,2]. In the dipole approximation, SHG is forbidden in the bulk of a medium having inversion symmetry, while at the surface inversion symmetry is broken and SHG is allowed. Despite this fundamental basis for the surface sensitivity of the SHG process, the method has been primarily employed in studying planar surfaces. Recent experiments have, however, demonstrated the utility of the approach for probing the surfaces of particles of down to submicron dimensions [3] and suggest a much wider range of application for the technique. At present, the theoretical description of the SHG process from nonplanar surfaces is relatively undeveloped. In particular, even for the simplest limiting case of SHG from the surface of a small sphere of centrosymmetric and isotropic material, no general theoretical description has been given. It is the purpose of this Letter to present the corresponding electromagnetic theory of second-harmonic (SH) scattering.

A distinctive feature of the process of the SH Rayleigh scattering (SHRS) lies in the role of cancellation of the radiation from different parts of the sphere. For linear Rayleigh scattering (LRS), the radiation process occurs without any significant phase shift or cancellation for a sphere of sufficiently small radius. The same circumstance applies to third-order nonlinear scattering processes [4,5]. For SHRS, however, the response vanishes in the dipole approximation owing to the presence of inversion symmetry [6]. In this work we develop a theory to describe the leading-order nonvanishing terms in a multipole expansion. Previously second-order nonlinear processes from spherical particles have been examined theoretically for a bulk nonlinearity [7,8] and for some special surface models [9,10]. Here we treat the interface in a general manner and derive a theory permitting an arbitrary response, in accordance with the model that has been successfully applied in nonlinear optical studies of adsorption, molecular orientation, spectroscopy, and dynamics at planar interfaces [1,2].

The analysis presented here reveals the leading-order contributions to SHRS arise from two sources: nonlocal excitation of an electric-dipole moment ($E1$) and local excitation of the electric-quadrupole moment ($E2$). The presence of these two sources and their distinct radiation patterns cause the SHRS process to differ significantly from that of LRS. In this Letter, we examine the nature of the radiation pattern for SHRS and present new selection rules, including the prohibition of nonlinear scattering along the forward and backward directions. From this analysis of the radiation process, we are able to give protocols for determining, as completely as possible, the surface nonlinear susceptibility tensor for the sphere. Consideration of the SHRS efficiency compared with that for a planar surface allows us to estimate the minimum particle size (radius $a \sim 5$ nm) for which SHRS scattering is expected to be readily observable. With respect to spectral characteristics, the basic variation of the scattered power in SHRS is found to scale with the frequency as ω^6, in contrast to the classic ω^4 dependence of LRS. In addition, we predict new resonances for metallic particles arising from excitation of both dipole and quadrupole surface plasmons.

The problem of SHRS is described schematically in Fig. 1. We wish to determine the SH radiation in the far field for nonlinear scattering from a sphere of radius a much less than the optical wavelength λ. We treat the nonlinear response of the sphere as a thin layer localized at the surface of the sphere and represented by a surface

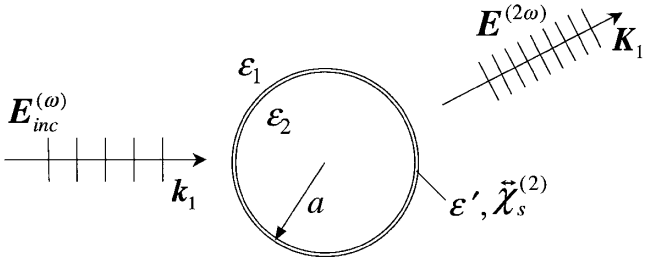

FIG. 1. Scheme for SH Rayleigh scattering by a sphere.

nonlinear source polarization $\mathbf{P}_s^{(2\omega)}$. The quantity $\mathbf{P}_s^{(2\omega)}$ is determined by the pump field $\mathbf{E}^{\prime(\omega)}$ present at the interface through $\mathbf{P}_s^{(2\omega)} = \overleftrightarrow{\chi}_s^{(2)}:\mathbf{E}^{\prime(\omega)}\mathbf{E}^{\prime(\omega)}$. No restriction is placed on the surface nonlinear susceptibility $\overleftrightarrow{\chi}_s^{(2)}$, other than the symmetry constraints appropriate for a sphere with a surface that is homogeneous and exhibits in-plane isotropy. With respect to the local coordinate system of parallel ($\parallel$) and perpendicular ($\perp$) directions, the allowed elements of $\overleftrightarrow{\chi}_s^{(2)}$ have the form of $\chi_{s,\perp\perp\perp}^{(2)}$, $\chi_{s,\perp\parallel\parallel}^{(2)}$, and $\chi_{s,\parallel\perp\parallel}^{(2)}$ [11]. We include an arbitrary isotropic linear dielectric response for the sphere (ε_2), the interface (ε'), and the lossless exterior region (ε_1). The incident excitation is taken as a plane wave, $\mathbf{E}_{inc}^{(\omega)}(\mathbf{r}) = E_0 \exp(i\mathbf{k}_1 \cdot \mathbf{r})\hat{\boldsymbol{\epsilon}}_0$, with a polarization state $\hat{\boldsymbol{\epsilon}}_0$ and wave vector $\mathbf{k}_1 = k[\varepsilon_1(\omega)]^{1/2}\hat{\mathbf{k}}_1 = (\omega/c)[\varepsilon_1(\omega)]^{1/2}\hat{\mathbf{k}}_1$.

We have solved this problem by recognizing that in the regions away from the interface, there is no nonlinear source. The general form of the electric fields may then be expressed as $\mathbf{E}^{(2\omega)} = \Sigma\{a_M^{lm} f_l(K_i r)\mathbf{X}_{lm}(\theta, \varphi) + a_E^{lm}\nabla \times [f_l(K_i r)\mathbf{X}_{lm}(\theta, \varphi)]/K_i\}$, where $f_l(K_i r) = \{j_l(K_i r), h_l^{(1)}(K_i r)\}$ is the appropriate spherical Bessel or Hankel function, respectively, $\mathbf{X}_{lm}(\theta, \varphi)$ are vector spherical harmonics, and $K_i = [\varepsilon_i(2\omega)]^{1/2}2k$ are the magnitudes of the SH wave vectors $\mathbf{K}_i$ outside ($i = 1$) or inside ($i = 2$) the sphere. The coefficients $\{a_M^{lm}, a_E^{lm}\}$ in the SH field expansion are obtained by applying boundary-matching conditions appropriate for a polarization sheet induced by the surface nonlinearity [2]. The formalism developed here may also be extended to SH scattering in the Mie regime (arbitrary sphere radius a), as will be treated elsewhere.

Following this procedure, we find for the radiated SH at location $\mathbf{r} = r\hat{\mathbf{n}}$ in the far field,

$$\mathbf{E}^{(2\omega)} = \frac{K_1^2 e^{iK_1 r}}{\varepsilon_1(2\omega) r}\left[\hat{\mathbf{n}} \times \left(\mathbf{p} - \frac{iK_1}{6}\mathbf{Q}(\hat{\mathbf{n}})\right)\right] \times \hat{\mathbf{n}}. \quad (1)$$

Here $\mathbf{p}$ and $\mathbf{Q}$ are the effective electric dipole and vector quadrupole moments, respectively, given by

$$\mathbf{p} = 8\pi i k_1 a^3 E_0^2 \chi_1 \hat{\mathbf{k}}_1(\hat{\boldsymbol{\epsilon}}_0 \cdot \hat{\boldsymbol{\epsilon}}_0)/15, \quad (2a)$$

$$\mathbf{Q}(\hat{\mathbf{n}}) = 16\pi a^3 E_0^2 \chi_2(\hat{\mathbf{n}} \cdot \hat{\boldsymbol{\epsilon}}_0)\hat{\boldsymbol{\epsilon}}_0/5, \quad (2b)$$

and quantities χ_1 and χ_2 are linear combinations of the elements of $\overleftrightarrow{\chi}_s^{(2)}$ with

$$\chi_l = \chi_{s,\perp\perp\perp}^{(2)}\mathcal{L}_l^{\perp\perp\perp} + \chi_{s,\perp\parallel\parallel}^{(2)}\mathcal{L}_l^{\perp\parallel\parallel} + \chi_{s,\parallel\perp\parallel}^{(2)}\mathcal{L}_l^{\parallel\perp\parallel}. \quad (3)$$

The coefficients $\mathcal{L}_l^{ijk}$, presented in Table I, account for the influence of the linear optical response of the system. They comprise products of the local-field factors $L_\parallel^{El}(\Omega) = (2l+1)\varepsilon_1(\Omega)/[l\varepsilon_2(\Omega) + (l+1)\varepsilon_1(\Omega)]$ and $L_\perp^{El}(\Omega) = \varepsilon_2(\Omega)L_\parallel^{El}(\Omega)/\varepsilon'(\Omega)$ for $E1$ ($l = 1$) and $E2$ ($l = 2$) modes at the fundamental ($\Omega = \omega$) and SH ($\Omega = 2\omega$) frequencies. The value of the magnetic local-field factor of $L_\parallel^{Ml} = 1$ results from the assumption of a spatially uniform magnetic permeability.

From Eqs. (1) and (2), we see that both electric-dipole and electric-quadrupole moments contribute to the leading-order response for SHRS. The comparable strength of these two terms arises from the fact that the electric-dipole moment is excited by the fundamental field through *nonlocal* interactions ($E1 + E2$ and $E1 + M1$), while the quadrupole moment is excited through a *local* interaction ($E1 + E1$). Magnetic-dipole ($M1$) emission, while of the same order, is absent because of the axial symmetry of the system. If we compare the features of SHRS with LRS, several differences may be readily identified. First, the SHRS radiation arises from two different modes ($E1$ and $E2$), while LRS is simply an $E1$ scattering process. Second, the $E1$ component in SHRS corresponds to a dipole aligned along the direction of the pump beam ($\hat{\mathbf{k}}_1$), rather than along the direction of the pump field ($\hat{\boldsymbol{\epsilon}}_0$), as in LRS. A further distinguishing feature for $E1$ emission in SHRS is that this mode of emission cannot occur for excitation by circularly polarized light.

To examine these emission properties, we calculate the radiated power per unit solid angle:

$$\frac{d\mathcal{P}_{2\omega}}{d\Omega_s} = \frac{cK_1^4}{2\pi[\varepsilon_1(2\omega)]^{3/2}}\left\{|\mathbf{p}|^2[1 - (\hat{\mathbf{n}} \cdot \hat{\mathbf{k}}_1)^2] + \left(\frac{K_1}{6}\right)^2|\mathbf{Q}(\hat{\mathbf{n}})|^2[1 - |\hat{\mathbf{n}} \cdot \hat{\boldsymbol{\epsilon}}_0|^2] + \frac{K_1}{3}\,\mathrm{Im}[(\hat{\mathbf{n}} \cdot \mathbf{p})(\hat{\mathbf{n}} \cdot \mathbf{Q}(\hat{\mathbf{n}}))^*]\right\}. \quad (4)$$

Figure 2 shows representative emission patterns for LRS (a), (e) and SHRS (b), (c), (d), (f). Figures 2(a)–2(d) correspond to linearly polarized excitation, while Figs. 2(e) and 2(f) correspond to circularly polarized pump radiation. For linearly polarized excitation, various radiation patterns may result. For pure dipole ($\chi_1 \neq 0$, $\chi_2 = 0$) or quadrupole ($\chi_1 = 0$, $\chi_2 \neq 0$) emission in (b) and (c), respectively, the radiation patterns are symmetric. In contrast, when both sources of radiation are present (χ_1, $\chi_2 \neq 0$), more complex and asymmetric radiation patterns result as, e.g., in Fig. 2(d) where $\chi_1 = [\varepsilon_1(2\omega)/\varepsilon_1(\omega)]\chi_2$. A selection rule that follows immediately from Eqs. (2) and (4) (and can be shown to hold for spheres of arbitrary size) is the lack of SH radiation emitted along the forward or backward directions.

In terms of application of SHRS to probe surface properties, $\overleftrightarrow{\chi}_s^{(2)}$ is the essential quantity linking electromagnetic response to the microscopic chemical and physical characterization of the system. We now consider its experimental determination. As we have demonstrated above, the SH radiation pattern is completely specified by the two coefficients χ_1 and χ_2, corresponding to the $E1$ and $E2$ emission terms. Thus, only two linear combinations of three allowed elements of $\overleftrightarrow{\chi}_s^{(2)}$ can be extracted [12]. Many schemes may be identified to find the

TABLE I. Effective field factors $\mathcal{L}_l^{ijk}$ in terms of the local-field factors $L_i^{\{E,M\}l}$.

l	$\mathcal{L}_l^{\perp\perp\perp}$	$\mathcal{L}_l^{\perp\parallel\parallel}$	$\mathcal{L}_l^{\parallel\perp\parallel}$
1	$L_\perp^{E1}(2\omega)L_\perp^{E1}(\omega)L_\perp^{E2}(\omega)$	$(3/2)L_\perp^{E1}(2\omega)L_\parallel^{E1}(\omega)L_\parallel^{E2}(\omega)$ + $(5/2)L_\perp^{E1}(2\omega)L_\parallel^{E1}(\omega)L_\parallel^{M1}(\omega)$	$-L_\parallel^{E1}(2\omega)L_\perp^{E1}(\omega)L_\parallel^{E2}(\omega)$ + $(3/2)L_\parallel^{E1}(2\omega)L_\perp^{E2}(\omega)L_\parallel^{E1}(\omega)$ − $(5/2)L_\parallel^{E1}(2\omega)L_\perp^{E1}(\omega)L_\parallel^{M1}(\omega)$
2	$L_\perp^{E2}(2\omega)L_\perp^{E1}(\omega)L_\perp^{E1}(\omega)$	$-L_\perp^{E2}(2\omega)L_\parallel^{E1}(\omega)L_\parallel^{E1}(\omega)$	$3L_\parallel^{E2}(2\omega)L_\perp^{E1}(\omega)L_\parallel^{E1}(\omega)$

experimentally accessible values of χ_1 and χ_2. One convenient approach is to record the SH power radiated at some scattering angle, $\theta(\neq 0, \pi/2)$, relative to $\hat{\mathbf{k}}_1$, as function of orientation of the polarization of a linearly polarized pump beam. By fitting such data to the functional form described by Eq. (4), one readily obtains the quantities $|\chi_1|$, $|\chi_2|$, and their relative phase. Note that to extract $|\chi_2|$ alone, one may employ a circularly polarized pump radiation, for which $E1$ emission is absent.

The strength of the SHRS process is of considerable importance from the experimental viewpoint: Since the nonlinear response arises from a surface layer in the presence of cancellation effects, one may expect relatively weak SH signals. In view of this situation, we examine the radiation efficiency for SHRS and apply this result to infer a typical range of experimentally accessible particle sizes. Experimentally, one can collect the SH radiation emitted into a large solid angle ($\approx$1 steradian). In this case, Eqs. (2) and (4) yield a scattered SH power from a particle of $\mathcal{P}_{2\omega} \approx cE_0^4|\chi_{sp}|^2(ka)^6$, where χ_{sp} is the effective nonlinear response. The corresponding expression for a planar interface may be written as $\mathcal{P}_{2\omega}^{pl} \approx cE_0^4|\chi_{pl}|^2k^2A_{pl}$, where A_{pl} is the irradiated area of the plane [2]. Consequently, the ratio η of the radiated SH power from a dilute collection of N spheres and to that from a planar interface is given by $\eta \equiv N\mathcal{P}_{2\omega}/\mathcal{P}_{2\omega}^{pl} \approx (ka)^4(|\chi_{sp}|^2A_{sp})/(|\chi_{pl}|^2A_{pl})$, where $A_{sp} = 4N\pi a^2$ is the aggregate area of the spheres. If we are able to probe a collection of particles with an aggregate area $A_{sp} \gtrsim A_{pl}$, then $\eta \gtrsim (ka)^4$ results for $|\chi_{sp}| \approx |\chi_{pl}|$. With current experimental techniques, one might reasonably assume that SH signals as small as 10^{-4} from that of a planar surface can be measured, corresponding to $\eta \approx 10^{-4}$ or $(ka) \lesssim 0.1$. This suggests that SHRS should be suitable for examining particles with radii $a \lesssim 5$ nm.

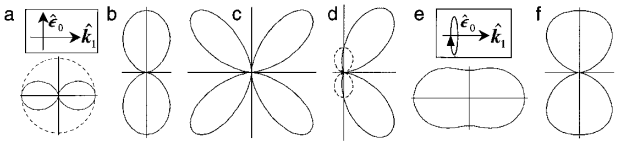

FIG. 2. Linear (a) and SH (b),(c),(d) radiation patterns excited by a linearly polarized light [(a), inset] for ($\chi_1 \neq 0$, $\chi_2 = 0$), ($\chi_1 = 0$, $\chi_2 \neq 0$), and [$\chi_1 = \chi_2\varepsilon_1(2\omega)/\varepsilon_1(\omega)$], respectively. The solid (dashed) lines describe scattering in a plane parallel (perpendicular) to the polarization of the incident light. Linear (e) and SH (f) radiation for circularly polarized excitation [(e), inset]. It should be noted that (b), (e), and (f) are solids of revolution about $\hat{\mathbf{k}}_1$, while (c) is a solid of revolution about $\hat{\boldsymbol{\epsilon}}_0$.

The final issue that we address is the spectral response of the SHRS process. Let us first consider the behavior for SHRS when all of the optical response, both linear and nonlinear, of the sphere may be considered as frequency independent. We then find from Eqs. (2) and (4) that the scattered SH power scales as ω^6. This contrasts with the well-known ω^4 behavior for LRS. This dependence will be modified by the inherent frequency dependence of $\overleftrightarrow{\chi}_s^{(2)}$. In addition, the linear optical response of the dielectric media as incorporated into the local-field factors may strongly influence the SH radiation. In particular, for materials with a metallic dielectric response with $\mathrm{Re}[\varepsilon_2] < 0$, new surface resonance modes are expected. These Fröhlich modes of the sphere occur when the real parts of the denominators of the local-field factors $L_\parallel^{El}$ vanish, i.e., $\mathrm{Re}[l\varepsilon_2(\Omega)] + (l+1)\varepsilon_1(\Omega) = 0$. Both the $l = 1$ and $l = 2$ modes may be resonantly enhanced by single- ($\Omega = \omega$) or two-photon ($\Omega = 2\omega$) processes. This leads to the presence of resonance enhancement in the SH scattering process at the four distinct frequencies where the resonance condition above is satisfied.

Within the Drude model of the dielectric response with $\varepsilon_2 = 1 - \omega_p^2/[\omega(\omega + i\gamma_p)]$, the resonance condition yields, for $\varepsilon_1 = 1$, dipole plasmon resonances at frequencies $\{\omega_p/\sqrt{3},\ \omega_p/\sqrt{12}\}$ and quadrupole plasmon resonances at frequencies $\{\omega_p\sqrt{2/5},\ \omega_p/\sqrt{10}\}$. We illustrate this behavior for a Drude model of aluminum. We take the surface nonlinearity to be dominated by $\chi_{s,\perp\perp\perp}^{(2)}$ and make use of bulk Drude parameters of $\hbar\omega_p \approx 15.55$ eV and $\hbar\gamma_p \approx 0.49$ eV, inferred from the experimental values for $\varepsilon_2(=\varepsilon')$ [13]. Figure 3 shows the spectral dependence of the enhancement in the total radiated power for metal spheres of radii $a = 2.5$, 5, and 10 nm relative to that from a spherical shell of fixed 2.5-nm radius. With respect to the size dependence of the response, the dominant characteristic arises from the scaling $\mathcal{P}_{2\omega} \propto a^6$ predicted by the electromagnetic theory developed in this Letter. We have also included two additional factors that alter the spectral characteristics as a function of particle radius: a finite-size correction for the plasmon resonance condition, which shifts the resonance frequencies to lower values with increasing size [14]; and a phenomenological modification of the metal dielectric response to account for surface scattering of the conduction electrons, which

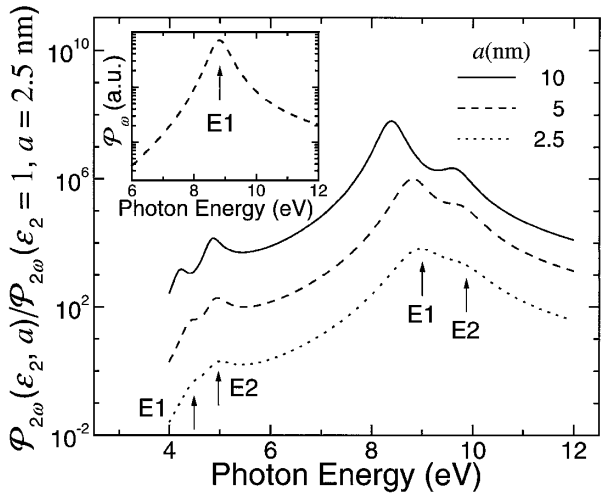

FIG. 3. Main panel: Spectral dependence of the radiated SH power, $\mathcal{P}_{2\omega}$, for linearly polarized excitation for metal spheres of radii $a = 2.5$, 5, and 10 nm. The power is plotted relative to that for a 2.5-nm-radius shell with the same surface nonlinear response ($\chi^{(2)}_{s,\perp\perp\perp}$) as that of the metal. Inset: Spectral dependence of $\mathcal{P}_\omega$ for linear scattering from metal spheres of radius $a = 5$ nm.

broadens the resonance features with decreasing size [15]. Although these effects alter the spectral profile somewhat, the principal features can still be identified as the four predicted plasmon resonances. The strong single-photon resonances are seen near photon energies of 9.0 and 9.8 eV and weaker two-photon resonances are present near 4.5 and 4.9 eV. LRS, on the other hand, exhibits only a single dipole plasmon peak near 9.0 eV [Fig. 3 (inset)]. In addition to the possibility for spectroscopic studies of both dipole and quadrupole plasmons afforded by SHRS, it should be noted that exploitation of those pronounced resonances significantly enhance the detection sensitivity for suitable particles.

Funding for this work was provided by the National Science Foundation through the Columbia EMSI program under Grant No. CHE-98-10367 and under Grant No. CHE-96-12294, and by the Division of Chemical Science, Office of Basic Energy Sciences of the DOE. We acknowledge helpful discussions with Professor Georg Reider and Professor Joel Gersten.

[1] J. F. McGilp, Prog. Surf. Sci. **49**, 1 (1995); K. B. Eisenthal, Chem. Rev. **96**, 1343 (1996); Y. R. Shen, Solid State Commun. **102**, 221 (1997), and references therein.

[2] T. F. Heinz, in *Nonlinear Surface Electromagnetic Phenomena*, edited by H.-E. Ponath and G. I. Stegeman (North-Holland, Amsterdam, 1991), p. 353.

[3] H. Wang *et al.*, Chem. Phys. Lett. **259**, 15 (1996); A. Srivastava and K. B. Eisenthal, Chem. Phys. Lett. **292**, 345 (1998); J. M. Hartings *et al.*, Chem. Phys. Lett. **281**, 389 (1997).

[4] See review articles by C. Flytzanis *et al.*, Prog. Opt. **29**, 321 (1991); U. Kreibig, in *Handbook of Optical Properties II*, edited by R. E. Hummel and P. Wißmann (CRC, Boca Raton, 1997), p. 145; R. F. Haglund, Jr., *ibid.*, p. 191; J. L. Cheung, J. M. Hartings, and R. K. Chang, *ibid.*, p. 233.

[5] U. Kreibig and M. Vollmer, *Optical Properties of Metal Clusters* (Springer-Verlag, Berlin, 1995).

[6] This work should be contrasted with SHG from fluctuations in molecular ensembles as in the work of R. W. Terhune, P. D. Maker, and C. M. Savage, Phys. Rev. Lett. **14**, 681 (1965). It also differs from SHG by small noncentrosymmetric structures, such as supported particles: O. A. Aktsipetrov *et al.*, Phys. Rev. B **51**, 17 591 (1995); T. Götz *et al.*, Appl. Phys. A **60**, 607 (1995); C. P. Collier *et al.*, Science **277**, 1978 (1997); J.-H. Klein-Wiele *et al.*, Phys. Rev. Lett. **80**, 45 (1998); B. Lamprecht *et al.*, Appl. Phys. B **68**, 419 (1999).

[7] G. S. Agarwal and S. S. Jha, Solid State Commun. **41**, 499 (1982).

[8] X. M. Hua and J. I. Gersten, Phys. Rev. B **33**, 3756 (1986).

[9] D. Östling, P. Stampfli, and K. H. Bennemann, Z. Phys. D **28**, 169 (1993).

[10] J. Martorell, R. Vilaseca, and R. Corbalán, Phys. Rev. A **55**, 4520 (1997).

[11] A nonlocal bulk nonlinear source polarization of the form $\mathbf{P}^{(2\omega)}_{\mathrm{bulk}} = \gamma\nabla(\mathbf{E}^{(\omega)} \cdot \mathbf{E}^{(\omega)})$ may also be readily incorporated into the model and all relations below through the substitutions of $\chi^{(2)}_{s,\perp\perp\perp} \rightarrow \chi^{(2)\mathrm{eff}}_{\perp\perp\perp}$ and $\chi^{(2)}_{s,\perp\parallel\parallel} \rightarrow \chi^{(2)\mathrm{eff}}_{\perp\parallel\parallel}$ with $\chi^{(2)\mathrm{eff}}_{\perp\perp\perp} = \chi^{(2)}_{s,\perp\perp\perp} + \gamma\ell(2\omega)[\ell(\omega)]^2$, $\chi^{(2)\mathrm{eff}}_{\perp\parallel\parallel} = \chi^{(2)}_{s,\perp\parallel\parallel} + \gamma\ell(2\omega)$, and $\ell(\Omega) = [\varepsilon'(\Omega)/\varepsilon_2(\Omega)]$.

[12] In contrast, for a planar surface, each of these tensor elements can be deduced experimentally. See, for example, Ref. [2].

[13] D. Y. Smith, E. Shiles, and M. Inokuti, in *Handbook of Optical Constants of Solids*, edited by E. D. Palik (Academic, Orlando, 1985), p. 369.

[14] As discussed in Ref. [7], if we consider the finite radius of the sphere, we may write more accurate plasmon resonance conditions $\mathrm{Re}[l\varepsilon_2(\Omega)] + (l + 1 + \Delta)\varepsilon_1(\Omega) = 0$, where $\Delta = [2(l + 1)(2l + 1)]/[l(2l - 1)(2l + 3)]x^2$ and $x = \{k_1 a, K_1 a\}$ corresponding to $\Omega = \{\omega, 2\omega\}$.

[15] The Drude damping constant is taken as $\gamma_p = \gamma_{\mathrm{bulk}} + Av_F/a$, where $\gamma_{\mathrm{bulk}} = 0.49$ eV is the parameter for the bulk metal, $v_F = 2 \times 10^8$ cm/s is the Fermi velocity, and A is a model-dependent parameter, which, for illustration, we set equal to 1 (see Ref. [5]).